HHS Public Access

Author manuscript

Brain Behav Immun. Author manuscript; available in PMC 2019 February 19.

Published in final edited form as:

Brain Behav Immun. 2018 January ; 67: 42–46. doi:10.1016/j.bbi.2017.08.003.

Corticosterone potentiates DFP-induced neuroinflammation and affects high-order diffusion imaging in a rat model of Gulf War Illness

Bang-Bon Koo[a,*,1], **Lindsay T. Michalovicz**[b,1], **Samantha Calderazzo**[a], **Kimberly A. Kelly**[b], **Kimberly Sullivan**[c], **Ronald J. Killiany**[a], and **James P. O'Callaghan**[b]

[a]School of Medicine, Boston University, Boston, MA, USA

[b]Health Effects Laboratory Division, Center for Disease Control and Prevention – National Institute for Occupational Safety and Health, Morgantown, WV, USA

[c]School of Public Health, Boston University, Boston, MA, USA

Abstract

Veterans of the 1991 Gulf War were potentially exposed to a variety of toxic chemicals, including sarin nerve agent and pesticides, which have been suspected to be involved in the development of Gulf War Illness (GWI). Several of these exposures cause a neuroinflammatory response in mice, which may serve as a basis for the sickness behavior-like symptoms seen in veterans with GWI. Furthermore, conditions mimicking the physiological stress experienced during the war can exacerbate this effect. While neuroinflammation has been observed post-exposure using animal models, it remains a challenge to evaluate neuroinflammation and its associated cellular and molecular changes *in vivo* in veterans with GWI. Here, we evaluated neuroimmune-associated alterations in intact brains, applying our existing GWI mouse model to rats, by exposing them to 4 days of corticosterone (CORT; 200 mg/L in the drinking water), to mimic high physiological stress, followed by a single injection of the sarin nerve agent surrogate, diisopropyl fluorophosphate (DFP; 1.5 mg/kg, i.p.). Then, we evaluated the neuroinflammatory responses using qPCR of cytokine mRNA and also examined brain structure with a novel high-order diffusion MRI. We found a CORT-enhancement of DFP-induced neuroinflammation, extending our mouse GWI model to the rat. High order diffusion MRI revealed different patterns among the different treatment groups. Particularly, while the CORT + DFP rats had more restricted spatial patterns in the hippocampus and the hypothalamus, the highest and most wide-spread differences were shown in DFP-treated rats compared to the controls in the thalamus, the amygdala, the piriform cortex and the ventral tegmental area. The association of these diffusion changes with neuroinflammatory cytokine expression indicates the potential for GW-relevant exposures to result in connectivity changes in the brain. By transferring this high order diffusion MRI into *in vivo* imaging in veterans with GWI, we can achieve further insights on the trajectories of the neuroimmune response over time and its impacts on behavior and potential neurological damage.

[*]Corresponding author at: Anatomy and Neurobiology, Boston University School of Medicine, Boston, MA 02118, USA. bbkoo@bu.edu (B.-B. Koo).

[1]These authors contributed equally to the work.

Keywords

Neuroimmune response; Diffusion MRI; Neuroinflammation; Gulf War Illness; Rat model; Cytokine; Corticosterone; Diisopropyl fluorophosphate; Rat model

1. Introduction

More than 25 years after the 1991 Gulf War, nearly one-third of the 697,000 U.S. troops who served continue to suffer from a complex, multi-symptom illness that is not well-explained by established medical or psychiatric diagnoses (White et al., 2016). The similarity of the symptoms associated with Gulf War Illness (GWI) to the classic symptoms of sickness behavior, including fatigue, chronic pain, memory complaints, and headaches, has high-lighted the possibility for GWI to be driven by underlying neuroinflammation (Dantzer and Kelley (2007)).

DoD modeling estimates 100,000 U.S. troops were potentially exposed to low level sarin and studies have found a potential impact of sarin in veterans with GWI (White et al., 2016). Accordingly, we developed a GWI mouse model incorporating exogenous corticosterone (CORT), to mimic physiological stress, and acute exposure to diisopropyl fluorophosphate (DFP), to mimic sarin nerve agent exposure experienced by GW veterans. This paradigm resulted in a marked brain-wide neuroinflammatory response in the absence of evidence of brain damage (O'Callaghan et al., 2015), highlighting the potential for these exposures to contribute to an underlying neuroinflammatory condition in GWI. In addition to mimicking sarin, DFP shares chemical characteristics with other irreversible acetylcholinesterase, organophosphate compounds that veterans were exposed to during the Gulf War, like the insecticides chlorpyrifos and dichlorvos. As such, we have demonstrated the potential for both DFP, as a sarin surrogate, and chlorpyrifos to instigate similar neuroinflammatory responses following CORT pretreatment (Locker et al., 2017), supporting a role for these classes of compounds in the development of GWI.

To draw an in-depth relationship between altered neuroinflammatory response and sickness behavior shown in veterans with GWI, it is important to have a monitoring method which is minimally invasive and allows for the combined evaluation of immuno-logical and neurological consequences of the toxic insults. Currently, there are different ways to examine neuroinflammatory responses *in vivo*. Measuring cytokine levels in CSF (Lenzlinger et al., 2004) may allow for the identification of proinflammatory markers in GWI. Also, positron emission tomography (PET) imaging can offer brain physiological information in GWI (Yehuda et al., 2010). However, the high invasiveness of lumbar puncture to obtain CSF and the costliness and insensitivity of PET (e.g., see Vivash and O'Brien, 2016) creates limits to the usefulness of these methods to address neuroinflammation in veterans with GWI. In order to bridge the animal to human extrapolation gap, magnetic resonance imaging (MRI) has been used to assess neural structural changes in association with an altered immune response, such as that proposed to underlie GWI. Morphometric MRI analysis of veterans with GWI confirmed overall reduction in the grey matter (GM) (Chao et al., 2010) and white matter (WM) (Heaton et al.,

2007; Chao et al., 2011), as well as a reduction in hippocampal and cortical GM volumes compared to healthy veterans (Chao et al., 2010). These regional morphometric changes have been tied to alterations in brain connectivity using diffusion MRI (Rayhan et al., 2013, Chao et al., 2011). Higher axial diffusivity measures have been reported in some WM major fiber pathways in the brains of GWI-suffering veterans. These findings may indicate that there are focal spots primarily involved in illness propagation in the brain; specifically, diffusion mapping may identify underlying structural and connectivity changes between brain cells (Anwander et al., 2010; McNab et al., 2013; Leuze et al., 2012).

2. Materials and methods

In this study, we expanded our established GWI mouse model (O'Callaghan et al., 2015; Locker et al., 2017) by exposing adult male Sprague Dawley rats (Hilltop Lab Animals, Scottdale, PA, USA) to CORT in the drinking water (200 mg/L in 0.6% EtOH) for 4 days, followed by a single injection of DFP (1.5 mg/kg, i.p.). Rats were sacrificed 6 h post-DFP by either decapitation for the evaluation of cortex cytokine mRNA (n = 5 rats/group), or by a fatal dose of pentobarbital-based euthanasia solution (Fatal Plus; 300 mg/kg, i.p.) followed by transcardial perfusion with 0.9% saline and fixation with 4% paraformaldehyde (n = 5 rats/group) for MRI. Total RNA from the frontal region of one cortical hemisphere was isolated as previously described (Locker et al., 2017). Real-time PCR analysis of the housekeeping gene, glyceraldehyde-3-phosphate dehydrogenase (GAPDH), and of the proinflammatory mediators, TNFα, IL-6, CCL2, IL-1β, leukemia inhibitor factor (LIF), and oncostatin M (OSM) was performed in an ABI7500 Real-Time PCR System (Thermo Fisher Scientific, Waltham, MA, USA) in combination with TaqMan® chemistry as previously described (Locker et al., 2017). Relative quantification of gene expression was performed using the comparative threshold ($\Delta\Delta C_T$) method. Changes in mRNA expression levels were calculated after normalization to GAPDH. The ratios obtained after normalization are expressed as fold change over corresponding saline-treated con- trols and two-way ANOVAs (pretreatment [water or CORT]× exposure [saline or DFP]; $p \leq 0.05$) were conducted on log transformed values using SigmaPlot v12.5 (Systat Software, Inc., San Jose, CA, USA). If statistical significance was detected between groups by two-way ANOVA, then Bonferroni post hoc analysis (statistical significance, $p \leq 0.05$) was performed to evaluate the statistical significance of all pairwise multiple comparisons. For diffusion MRI imaging analysis, paraformaldehyde-perfused brains were scanned for 10 h on a 4.7 T Bruker MRI with an applied diffusion weighted spin-echo echo planar imaging sequence (SE-EPI) with the following parameters: 500 lm isotropic voxel, coronal slice acquisition with 515 independent diffusion gradient directions using b-values up to 40,000 s/mm^2 (Wedeen et al., 2008). For each brain, five non-diffusion weighted (b0) images were averaged to perform pre-processing of the raw diffusion scans and a modified in-house processing pipeline (Koo et al., 2013) was used to perform sequential pre-processing steps on the data. Q-space imaging method (Yeh et al., 2010) were used for the reconstruction of diffusion parameters. Three dimensional probability information on the diffusion displacement was calculated in each voxel in the brain scans and then formed the spin distribution function. Micro-scale diffusivity was modeled for partial diffusion encoding length based on the weighted sum of partial spin distributions below upper bound of the diffusion displacement (Yeh et al., 2016).

In this study, we applied 2 μm, 10 μm and 20 μm upper bounds for calculating the micro-scale diffusivity maps. We also calculated generalized fractional anisotropy (GFA) based on the spin distribution in q-space reconstruction. GFA has been used for quantifying microstructural integrity (similar to fractional anisotropy in diffusion tensor imaging) for q-space diffusion imaging. From the pre-processing, all diffusion indices on each brain were nonlinearly transformed to the atlas space to perform group-level statistics and all brain images were smoothed based on the Gaussian kernel (1.5 mm FWHM). Regional impacts were highlighted using unpaired group statistics between controls and the other groups (CORT, DFP, CORT+DFP) per each diffusion index separately. We conducted permutation-based random effect corrections for multiple comparison corrections with 5000 permutations to correct for possible random effects. Voxels with significant differences were defined by $p < 0.05$ and significant clusters were then mapped to the atlas to confirm anatomical information.

3. Results

Similar to our mouse model (O'Callaghan et al., 2015), we found that not only does DFP alone increase the expression of several of the evaluated genes, but also that prior CORT exposure significantly exacerbated this response (Fig. 1). The micro-scale diffusivity mapping successfully differentiated either CORT and/or DFP responses in the brain (Fig. 2A, first row) with higher micro-scale diffusivity values in the CORT, DFP, and CORT+DFP groups compared to controls (Fig. 2B). Among the diffusion upper bounds evaluated (Fig. 2A, second row), the 10 lm partial diffusion encoding revealed more statistically significant group differences, identifying more widespread clusters covering the hippocampus and outer cortices in the CORT+DFP group over controls. Furthermore, while the CORT+DFP treated brains had more restricted patterns in the hippocampus and the hypothalamus, the highest and most widespread differences were shown in the thalamus, amygdala, piri-form cortex and ventral tegmental area of DFP-treated (corrected $p < 0.001$) followed by CORT-treated (corrected $p<0.01$) rats. Generalized fractional anisotropy (GFA) revealed less significant differences compared to the micro-scale diffusivity measures. Differences between the controls and DFP-treated brains had spatial pattern overlap with the micro-scale diffusivity mapping results in regions including the medial frontal and hippocampal regions (Fig. 2 third row), whereas CORT and CORT+DFP had distinct patterns compared to their micro-scale mapping results.

4. Discussion

Here, we have shown that the CORT-enhanced DFP-induced neuroinflammatory model developed for the mouse (O'Callaghan et al., 2015) can be extended to the rat and that diffusion MRI can successfully differentiate between the exposure conditions of this GWI model. We have demonstrated previously that our model of GWI is an instigation of neuroinflammation without evidence of brain damage. This has been shown previously with immunohisto-chemistry at relevant, short-term time points in mice (O'Callaghan et al., 2015) through an absence of positive silver stain and Fluoro-Jade markers for degenerating neurons, as well as a lack of changes in microglia or astrocytes. Similar results have been confirmed in our rat model at comparable time points (unpublished data). Therefore, at this

early time point, we have shown the neuroinflammatory potential of DFP and CORT+DFP exposure in the absence of damage. Furthermore, what we have demonstrated here is that this neuroinflammatory response results in subtle, but differentiable changes in diffusion MRI, which highlights the ability to detect inflammatory-induced changes in MRI patterns early and without the requirement of severe damage to the brain tissue. Recent studies using similar diffusion parameters also reported successful discrimination of microstructural changes in neuronal or glial cell elements (Johnson et al., 2014, Blumenfeld-Katzir et al., 2011). In addition, high-order diffusion MRI successfully captured statistically significant changes in diffusion indices in a rat model of mild traumatic brain injury as early as 2 h post-injury (Zhuo et al., 2012). While the current study evaluates early time points in relation to a chronic illness, these conditions model what we would hypothesize to have been experienced immediately following exposure in theater or the proposed initiating events of GWI. Various studies of long-term time points that are more closely relevant to the current condition of veterans with GWI are on-going in our rodent models of GWI. Future studies will aim to address the potential for this model of “in theater” exposure conditions to progress into the chronic condition we associate with GWI and evaluate how these early diffusion changes may correlate or predict MRI results in a long-term model of GWI.

By using higher-order diffusion MRI, the limitations in the ability to assess minor changes in subcellular components typically associated with clinical diffusion MRI (typically, around $b = 1000$ s/mm^2) can be avoided (Palacios et al., 2014, Wang et al., 2015). Furthermore, the addition of GFA mapping, which is a common index for assessing the intactness of white matter tracts, revealed different patterns than the micro-scale assessments, indicating that exposure to DFP may affect micro-structural changes in major cortical connections. While more work is needed to understand how these patterns directly correlate to neuroinflammation, the identification of these unique MRI patterns in our GWI rodent model indicates the potential for underlying neuroinflammation to be associated with morphological and/or connectivity changes in neurons and glia. Considering that published and preliminary immunohistochemistry studies in both mice (O’Callaghan et al., 2015) and rats (unpublished data) have indicated no major, macroscopic changes indicative of cell death or morphological alterations of neurons or glia, we would hypothesize that these diffusivity changes are the result of more microscale changes in morphology like the arborization of dendrites or glial processes. These would be subtle changes in response to neuroinflammation that do not result in traditional, damage-induced “activation” of either microglia or astrocytes. Overall, since the high-order diffusion imaging protocol is also available to 3T clinical scanners, these results help to establish high-order diffusion MRI as a means to evaluate subtle ultra-structural changes in neural cells, which may be associated with *in vivo* neuroinflammation, in veterans with GWI.

Acknowledgments

Drs. Koo and Michalovicz contributed equally to this work. We appreciate the excellent technical assistance provided by Samantha Calderazzo, Brenda K. Billig and Christopher M. Felton. This work is supported by a department of Defense CDMRP GWI consortium award (W81XWH-13-2-0072). Disclaimer: The findings and conclusions in this report are those of the author(s) and do not necessarily represent the views of the National Institute for Occupational Safety and Health. This work was supported by the Assistant Secretary of Defense for Health Affairs, through the Gulf War Illness Research Program, GW120037. Opinions, interpretations, conclusions and recommendations are those of the author and are not necessarily endorsed by the Department of Defense.

References

Anwander A, Pampel A, Knosche TR, 2010 In vivo measurement of cortical anisotropy by diffusion weighted imaging correlates with cortex type. Proc. Int. Soc. Magn. Reson. Med 18, 109.

Blumenfeld-Katzir T, Pasternak O, Dagan M, Assaf Y, 2011 Diffusion MRI of structural brain plasticity induced by a learning and memory task. PLoS ONE 6 (6), e20678. [PubMed: 21701690]

Chao LL, Abadjian L, Hlavin J, Meyerhoff DJ, Weiner MW, 2011 Effects of low-level sarin and cyclosarin exposure and Gulf War Illness on brain structure and function: a study at 4T. NeuroToxicol. 32 (6), 814–822.

Chao LL, Rothlind JC, Cardenas VA, Meyerhoff DJ, Weiner MW, 2010. Effects of low-level exposure to sarin and cyclosarin during the 1991 Gulf War on brain function and brain structure in US veterans. NeuroToxicol. 31 (5), 493–501. 10.1016/j.neuro.2010.05.006.

Dantzer R, Kelley KW, 2007 Twenty years of research on cytokine-induced sickness behavior. Brain Behav. Immun 21 (2), 153–160. [PubMed: 17088043]

Heaton KJ, Palumbo CL, Proctor SP, Killiany RJ, Yurgelun- Todd DA, White RF, 2007 Quantitative magnetic resonance brain imaging in US army veterans of the 1991 Gulf War potentially exposed to sarin and cyclosarin. Neurotoxicology 28 (4), 761–769. [PubMed: 17485118]

Johnson GA, Calabrese E, Little PB, Hedlund L, Qi Y, Badea A, 2014 Quantitative mapping of trimethyltin injury in the rat brain using magnetic resonance histology. Neurotoxicology 42, 12–23. [PubMed: 24631313]

Koo B-B, Oblak AL, Zhao Y, Farris CW, Bowley B, Rosene DL, Killiany RJ, 2013 Hippocampal network connections account for differences in memory performance in the middle-aged rhesus monkey. Hippocampus 23 (12), 1179–1188. [PubMed: 23780752]

Lenzlinger PM, Hans VHJ, Joller-Jemelka HI, Trentz O, Morganti-Kossmann MC, Kossmann C, 2004 Markers for cell-mediated immune response are elevated in cerebrospinal fluid and serum after severe traumatic brain injury in humans. J. Neurotrauma 18 (5), 479–489.

Leuze CW, Anwander A, Bazin PL, Stüber C, Reimann K, Geyer S, Turner R, 2012 Layer specific intracortical connectivity revealed with diffusion MRI. Cereb. Cortex 24 (2), 328–339. [PubMed: 23099298]

Locker AR, Michalovicz LT, Kelly KA, Miller JV, Miller DB, O'Callaghan JP, 2017 Corticosterone primes the neuroinflammatory response to Gulf War Illness-relevant organophosphates independently of acetylcholinesterase inhibition. J. Neuorchem 10.1111/jnc.14071.

McNab JA, Polimeni JR, Wang R, Augustinack JC, Fujimoto K, Stevens A, Janssens T, Farivar R, Folkerth RD, Vanduffel W, Wald LL, 2013 Surface based analysis of diffusion orientation for identifying architectonic domains in the in vivo human cortex. NeuroImage 69, 87–100. [PubMed: 23247190]

O'Callaghan JP, Kelly KA, Locker AR, Miller DB, Lasley SM, 2015 Corticosterone primes the neuroinflammatory response to DFP in mice: potential animal model of Gulf War Illness. J. Neurochem 133 (5), 708–721. [PubMed: 25753028]

Palacios RDY, Verhoye M, Henningsen K, Wiborg O, Van der Linden A, 2014 Diffusion kurtosis imaging and high-resolution MRI demonstrate structural aberrations of caudate putamen and amygdala after chronic mild stress. PLoS ONE 9 (4), e95077. [PubMed: 24740310]

Rayhan RU, Stevens BW, Timbol CR, Adewuyi O, Walitt B, VanMeter JW, Baraniuk JN, 2013 Increased brain white matter axial diffusivity associated with fatigue, pain and hyperalgesia in Gulf War illness. PLoS ONE 8 (3), e58493. [PubMed: 23526988]

Vivash L, O'Brien TJ, 2016 Imaging microglial activation with TSPO PET: lighting up neurologic diseases? J. Nucl. Med 57 (2), 165–168. [PubMed: 26697963]

Wang Y, Sun P, Wang Q, Trinkaus K, Schmidt RE, Naismith RT, et al., 2015 Differentiation and quantification of inflammation, demyelination and axon injury or loss in multiple sclerosis. Brain 138 (5), 1223–1238. [PubMed: 25724201]

Wedeen R, Wang J, Schmahmann T, Benner W, Tseng G, Dai D, Pandya P, Hagmann Arceuil H de Crespigny A, 2008 Diffusion spectrum magnetic resonance imaging (DSI) tractography of crossing fibers. Neuroimage 41 (4), 1267–1277. [PubMed: 18495497]

White RF, Steele L, O'Callaghan JP, Sullivan K, Binns JH, Golomb BA, et al., 2016 Recent research on Gulf War illness and other health problems in veterans of the 1991 Gulf War: effects of toxicant exposures during deployment. Cortex 74, 449–475. [PubMed: 26493934]

Yeh FC, Wedeen VJ, Tseng WY, 2010 Generalized q-sampling imaging. IEEE Trans. Med. Imaging 29 (9), 1626–1635. [PubMed: 20304721]

Yeh FC, Liu L, Hitchens TK, Wu YL, 2016 Mapping immune cell infiltration using restricted diffusion MRI. Magn. Reson. Med 77 (2), 603–612. [PubMed: 26843524]

Yehuda R, Golier JA, Bierer LM, Mikhno A, Pratchett LC, Burton CL, et al., 2010 Hydrocortisone responsiveness in Gulf War veterans with PTSD: effects on ACTH, declarative memory hippocampal [18F]FDG uptake on PET. Psychiatry Res. 184 (2), 117–127. [PubMed: 20934312]

Zhuo J, Xu S, Proctor JL, Mullins RJ, Simon JZ, Fiskum G, Gullapalli RP, 2012 Diffusion kurtosis as an in vivo imaging marker for reactive astrogliosis in traumatic brain injury. Neuroimage 59 (1), 467–477. [PubMed: 21835250]

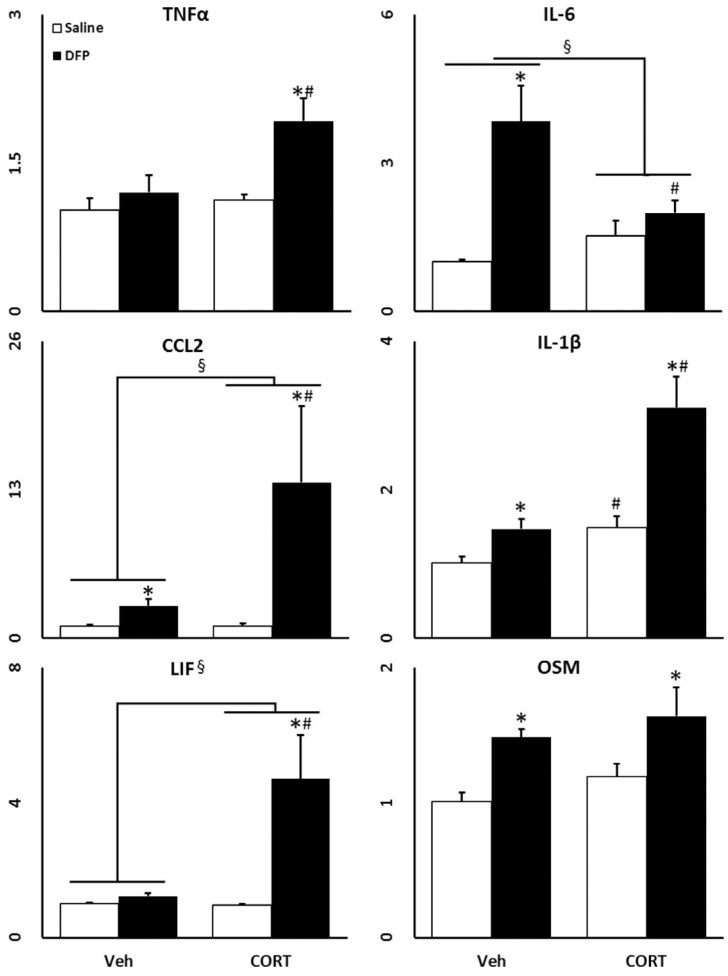

Fig. 1.

Chronic CORT exacerbates DFP induced inflammation in rats. Effects of chronic CORT pretreatment (200 mg/L 0.6% EtOH in drinking water for 4 days) on DFP (1.5 mg/kg, i.p.) induced neuroinflammation in the cortex at 6 h post DFP exposure is shown with TNFα, IL-6, CCL2, IL-1β, LIF, and OSM qPCR. Data represents mean ± SEM (n = 5 rats/group). Statistical significance of at least $p < 0.05$ is denoted by * as compared within pretreatment (vehicle or CORT), # as compared within exposure (saline or DFP), and § for a significant interaction between pretreatment and exposure.

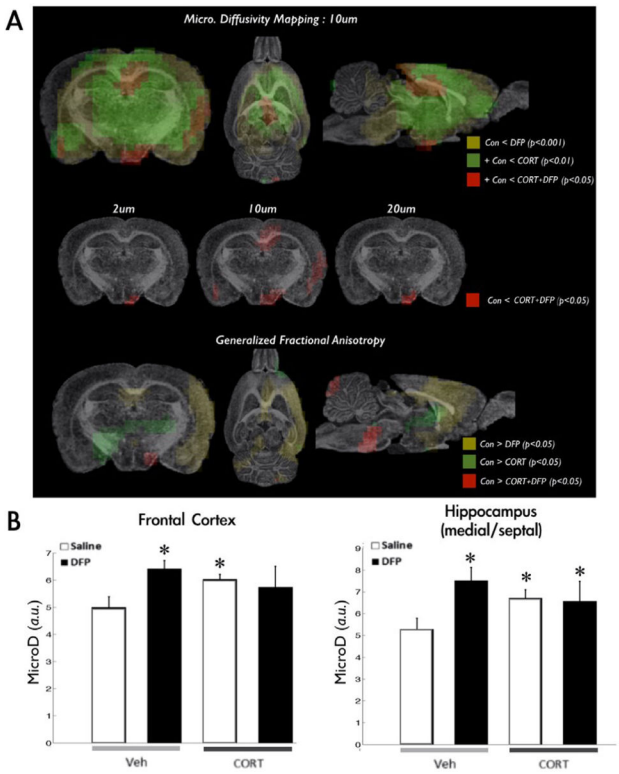

Fig. 2.

Microscale diffusivity mapping in CORT + DFP treated rats. Group differences in microscale diffusivity is shown in panel A. Statistically significant differences between controls and DFP treated rats are shown in the clusters with yellow color encodings. Green clusters are overlapped to the yellow clusters and indicates differences between controls and CORT-treated rats. Red clusters are overlapped to the previous two clusters and show differences between controls and CORT + DFP treated rats. We confirmed that diffusion encoding length at 10 lm had more sensitivity to detect statistically significant group differences in between controls and CORT + DFP treated rats as shown in the second row of panel A. Generalized fractional anisotropy maps revealed distinct patterns with lower statistical thresholds compared to the micro diffusivity maps (third row in panel A). Panel B shows quantification of micro diffusivities in the frontal cortex and the hippocampus. In both graphs, white and black bar in Veh section shows average micro-diffusivity value of each region of interest in saline and DFP accordingly. Also, white and black bar in CORT section shows average micro-diffusivity value of each region of interest in CORT and CORT + DFP. (For interpretation of the references to color in this figure legend, the reader is referred to the web version of this article.)